AD-A087 055 MARYLAND UNIV COLLEGE PARK DEPT OF PHYSICS AND ASTRONOMY F/6 20/7
A 1-D COMPUTER SIMULATION MODEL OF COLLECTIVE ION ACCELERATION --ETC(U)
MAY 79 A STERNLIEB, H S ULM N00014-80-C-0050
UNCLASSIFIED PUB-80-010 NL

1 of 1
AD
A087055

END
DATE
FILMED
9 80
DTIC

LEVEL

Plasma Preprint PL #80-002

ADA087055

A 1-D COMPUTER SIMULATION MODEL OF COLLECTIVE ION ACCELERATION BY LINEAR ELECTRON BEAMS

by

A. Sternlieb
Department of Physics and Astronomy
University of Maryland
College Park, Maryland 20742

and

Han S. Uhm
Naval Surface Weapons Center
White Oak, Silver Spring, Maryland 20910

Physics Publication Number 80-010
Technical Report Number 80-007

May 1979

Contract N00014-80-C-0050

UNIVERSITY OF MARYLAND
DEPARTMENT OF PHYSICS AND ASTRONOMY
COLLEGE PARK, MARYLAND

Plasma Preprint PL #80-00

A 1-D COMPUTER SIMULATION MODEL

OF COLLECTIVE ION ACCELERATION BY LINEAR ELECTRON BEAMS

by

A. Sternlieb
Department of Physics and Astronomy
University of Maryland
College Park, Maryland 20742

and

Han S. Uhm
Naval Surface Weapons Center
White Oak, Silver Spring, Maryland 20910

Physics Publication Number 80-010
Technical Report Number 80-007

May 1979

Contract # N00014-80-C-0050

A 1-D COMPUTER SIMULATION MODEL OF COLLECTIVE ION ACCELERATION BY LINEAR ELECTRON BEAMS

by

A. Sternlieb
Department of Physics and Astronomy
University of Maryland
College Park, Maryland 20742

and

Han S. Uhm
Naval Surface Weapons Center
White Oak, Silver Spring, Maryland 20910

17 pages

8 figures

COLLECTIVE ION ACCELERATION CODE

A. Sternlieb
Department of Physics and Astronomy
University of Maryland
College Park, Maryland 20742

ABSTRACT

A 1-d electrostatic and relativistic particle code has been built in order to simulate in a self-consistent way the time-dependent behavior of collective ion acceleration produced by linear electron beams injected into evacuated drift tubes. The simulation results agree with existing experimental and theoretical results by showing good current propagation and high ion energy gain in the presence of a well-localized plasma source at the e-beam injection boundary. Moreover, the simulations display an unexpected phenomenon, the appearance of short-lived regions of positive electrostatic potential ("virtual anodes") which together with the usual virtual cathodes, contribute to the ion acceleration mechanism. In the absence of a suitable analytical theory, it seems to us that the present computer model is an indispensable tool for reliable explanation and optimization of present and future collective ion acceleration experiments. Use of our model in laser-plasma experiments is suggested.

I. INTRODUCTION

In recent years, heavy ion beams have been considered as possible drivers in an inertial confinement fusion scheme, because of their good deposition characteristics and because of the already existing advanced accelerator technology, capable of high repetition rates [1]. However, a serious drawback is the high cost of these accelerators. A promising and possibly less expensive approach is the use of collective ion acceleration (CIA) as a source for heavy ion beams. In a typical CIA experiment a relativistic electron beam is injected into a drift tube in which an ion source is present. The ions which initially have negligible kinetic energy, are eventually accelerated by the collective electrostatic fields generated by the incoming electron beam. Basically, in this process long e-beam pulses are transformed into short energetic ion pulses.

The collective acceleration of protons and heavier ions by linear electron beams injected into initially evacuated drift tubes, has been investigated at several laboratories [2-5]. The ion source is produced either from an insulating anode or from a puffed-in gas, by an e-beam prepulse or possibly by laser irradiation. Reported experiments indicate that effective e-beam propagation and effective collective acceleration occur when the plasma source is initially well-confined to the anode. Collectively accelerated protons have been observed in these experiments with energies of up to 20 times the beam electron energy, and heavier ions (C, N, O, F, Cl) have been accelerated to energies of several MeV per nucleon.

In order to explain the CIA mechanism, it has been recently suggested [2,6] that some ions from the dense, anode-localized plasma source are trapped and accelerated by the electrostatic fields associated with a moving potential well of a depth comparable to the injected e-beam energy. An explicit relationship is given for the fastest ion energy as function of time, injected energy and current, ion mass and charge state, and drift tube length. The effect of the ion charge on the potential distribution is not taken into account. However, experiments indicate a strong coupling between electrons and ions during their propagation towards the downstream end of the drift tube (coherent movement is observed). This means that both electrons and ions may have comparable effects on the development of the electrostatic potential well.

Therefore, in spite of the success of the above theory in giving some crude evaluation of the maximum achievable ion energies, there is a critical need for a time-dependent model, in which ions and electrons are included in a self-consistent manner. In order to investigate the properties of the fully nonlinear ion acceleration mechanism we have built a one-dimensional relativistic particle simulation code, which includes the dynamic equations for the electrons and ions simultaneously. This should allow a more detailed assessment of the ion energy gain. Besides being the only means for a self-consistent time-dependent study of CIA, computer simulation allows for a multitude of diagnostics and a strict control of the system parameters. Once the acceleration mechanism is understood, we can determine the optimum system parameters for experiments planned at several laboratories [2-4], in order to accelerate ions to maximum energy and current.

In Section II, we describe the technical details of our simulation code. In Sec. III, we present preliminary simulation results and compare them with theory and experiments. In Sec. IV, we outline the main conclusions of this study.

II. THE SIMULATION CODE

A sketch of the simulated physical system is presented in Fig. 1. A relativistic electron beam, usually produced by a diode is injected into an initially evacuated drift tube, forming a virtual cathode (defined as the minimum of the potential well). If an unlimited, infinitely thin plasma layer is available at the injection site, ions will be emitted from the plasma source in a space-charge limited manner and will be accelerated by the virtual cathode towards the downstream end of the drift tube. Whenever the electric field at the injection boundary becomes negative, electrons will be emitted from the plasma source, instead of ions. The electrons and the ions in the drift tube are free to move under the effect of the self-consistent collective electric field generated by the net charge density distribution. The potential difference across the tube is assumed to be always zero, and the charge emission occurs due to the presence of the potential well generated by the incoming electron beam. The injected electrons have all the same velocity, corresponding to their relativistic energy. The emitted ions or electrons start with negligible kinetic energies. In the present code we assume the injected current and energy to be constant, although any time-dependence can be accomodated in our model. Both electrons and ions, emitted or injected into the drift tube are absorbed by the downstream side of the tube, once they reach it. This side of the drift tube is not assumed to emit particles, although this may happen in reality. Therefore, the electric field is strictly zero only at the injection boundary and at the minima of the potential well. Usually, the source of the injected electron beam is a relativistic diode, whose anode is identical with the injection boundary of the drift tube. Our code simulates the drift tube part of the system, with the e-beam current and energy externally given.

The physical parameters in the simulation are as follows: the e-beam energy,

$V_o(t)$; the e-beam current density, $J_e(t)$; the drift tube length, d; and the charge to mass ratio of the ions, q_i/m_i. The simulation parameters are: the space step, Δz; the time step, Δt; the number of particle records (half electrons, half ions), NREC; the number of particles per record, NBATCH; the number of cells in the system, NZ ($d = NZ \cdot \Delta z$); the number of particles to be emitted at each time step, NEMIT.

Our PIC code is $1\frac{2}{2}$ dimensional (z, v_z, v_r), electrostatic and relativistic. A flow chart of the simulation code is presented in Fig. 2. Initially, the code starts with a vacuum drift tube: $\rho(z) = 0$. The code solves the poisson equation $\nabla^2\phi(z) = -4\pi\rho(z)$, where $\phi(z)$ is the potential distribution, and $\rho(z)$ is the net charge distribution in the system. The boundary conditions are: $\phi(A1) = \phi(A2) = 0$, where A1 and A2 are the injection and the downstream boundaries, respectively. After finding $\phi(z)$, the electric field $E_z(z)$ is calculated from:

$$E_z(z) = [\phi(z) - \phi(z + \Delta z)]/\Delta z \ .$$

This gives $E_z(A1)$, the electric field at the injection boundary, before emission. Then we use the gaussian law for space charge limited emission at A1, in order to make the electric field equal to zero, at the emission boundary. If $E_z(A1)$ is positive, ions are emitted at A1, according to the relation:

$$Q_i^{emit}(A1) = E_z(A1)/4\pi A \quad ,$$

where Q_i^{emit} is the surface charge density of the emitted ions, and $A(= 1 - 0.5/NZ)$ is a correction factor aimed at matching the boundary conditions to the finite grid system. If $E_z(A1)$ is negative, electrons will be emitted at A1, (in addition to the injected electrons), given by the same expression:

$$Q_{el}^{emit}(A1) = E_z(A1)/4\pi A$$

The corresponding current densities are defined as:

$$J_i^{emit}(A1) = Q_i^{emit}(A1)/\Delta t$$

$$J_{el}^{emit}(A1) = Q_{el}^{emit}(A1)/\Delta t$$

The other current density components in the system are: $J_{el}^{abs}(A1)$, $J_{el}^{abs}(A2)$, $J_i^{abs}(A1)$, $J_i^{abs}(A2)$, where el = electrons, i = ions, abs = absorbed. No currents are assumed to be emitted at A2. Q_{el}^{inj} is the surface charge density of the injected electrons defined as:

$$Q_{el}^{inj} = -J_e^{inj}\Delta t/CMKS,$$

where CMKS converts amps to CGS units if J_e^{inj} is given in A/cm^2; J_e^{inj} is the injected electron current density.

Next, the electrostatic potential is modified to take into account the effect of the emitted and injected charges at A1. This is done by using a Green-like function which represents the correction to the potential due to one unit of surface charge density at A1. This function, $\Delta\phi_e$, does not alter the potential boundary values. It only makes the electric field equal to zero at the emitting electrode, A1. This correcting function is given by [8]:

$$\Delta\phi_e(z) \begin{cases} = -2\pi\Delta z(z-d)/d, & +\Delta z/2 \leq z \leq d \\ = -4\pi(\Delta z/2-d)/d, & -\Delta z/2 \leq z \leq \Delta z/2 \end{cases}$$

The corrected electrostatic potential function will then be:

$$\phi^c(z) = \phi(z) + [Q_i^{emit}(A1) + Q_{el}^{emit}(A1) + Q_{el}^{inj}(A1)] \cdot \Delta\phi_e(z)$$

The corrected electric field $E_z^c(z)$ is therefore given by:

$$E_z^c(z) = (1/\Delta z) \cdot [\phi^c(z) - \phi^c(z + \Delta z)],$$

which satisfies: $E_z^c(A1) = 0$.

The particles are then actually emitted into the system. The injected electrons have all the same longitudinal velocity, (no transverse momentum), given by:

$$v_z^e = c\sqrt{2\,\bar{V}_o(1 + 0.5\,\bar{V}_o)}\Big/(1 + \bar{V}_o),$$

where $\bar{V}_o = V_o/m_e c^2$, and initially they are placed according to:

$$z = 0.5 \cdot \text{random}\,(0,1) + \Delta t \cdot v_z^e/2\Delta z$$

The electric field $E_z^c(z)$ is then used to push the particles (relativistically for electrons or positrons, nonrelativistically for ions) to their new positions, during the time step Δt. The new charge distribution $\rho(z)$ is calculated by the usual grid-weighting method, and finally the code proceeds to the next time step.

Many diagnostics are built in the code for analyzing the electrostatic field and potential, the various current components and the energy spectra of the particles. Various options are available within this code, as follows:

(a) Ions can be emitted in various modes, corresponding to the experimental designs. For example, besides the space-charge limited emission mentioned above, ions can be emitted from a finite plasma source near the injection boundary, until the source is depleted.

(b) A delay can be allowed between the times of plasma source formation and electron beam injection.

(c) The potentials at A1 and A2 may not be equal. In fact, experiments have been done with $\phi(A1) = 0$ and $\phi(A2) = -V_o$.

(d) The injected electrons need not be mono-energetic, but can have a given velocity distribution function $f(v_e)$ (e.g. Maxwellian). This enables one to apply the code to the analysis of fast ions produced by the high energy tail of the electron distribution function generated in laser produced plasmas.

The choice of the simulation parameters should fulfill some basic requirements. First, the time step should be small enough to allow rapid time variations of the physical quantities. For example, we require $\Delta v_e < v_e^{max} (\lesssim c)$ at anytime, where v_e is the electron speed and c is the light speed. Taking the maximum possible value for the electric field (when the voltage between A1 and the virtual cathode spans across a few simulation cells) we get: $\Delta t < (\Delta z/V_o)(m_e c/e)$. This is formally similar to a Courant-type condition, $\Delta z > c\Delta t$, in which the fastest electrons are not allowed to travel over more than one cell during one time-step in order to correctly sample the space-varying field. In cases with high injected current densities, situations with high and rapidly space and time varying electric fields often occur. Thus, quite small time steps must be used in these cases. On the other hand, very short time steps cause prohibitively long computational times or large accumulation errors.

A separate condition exists on Δz, to ensure that the system can accomodate the highest physically attainable currents in the system. This condition poses an upper limit on Δz, which for a given d, determines the minimum number of simulation cells, NZ, to be used ($d = NZ \cdot \Delta z$) for given J_e^{inj}, V_o and d.

A different problem exists concerning the physical parameters of the simulations. In all our simulations, we use realistic values for J_e^{inj}, V_o and d. However, for m_i/m_e, we have chosen a value of 25, much lower than in the experiments. We do this in order to reduce the computational times to acceptable levels. A study of the scaling-up of the simulation results with m_i/m_e and other parameters is necessary. From preliminary results it seems that only the time scales are affected, while the final saturation values of current components and ion energies are relatively independent of m_i/m_e.

III. SIMULATION RESULTS

As a first test case, we performed a simulation with only the electrons present. The simulation parameters were the following: the injected e-beam current density, $J_e = 10\ KA/cm^2$; the energy, $V_o = 1$ MeV; $\Delta t = 1.5$ psec; $\Delta z = 0.07$ cm; NZ = 128 ($d = \Delta z \cdot NZ = 9.1$ cm). Initially, a deep potential well of 2-3 times V_o is formed which lasts for a few plasma periods. No electron current propagates during this period. Then, the potential stabilizes and the virtual cathode amplitude (defined as the minimum of the potential well) oscillates up and down in the steady state around a nearly constant position of $\approx$1 cm (Figs. 3,4). These oscillations have been suggested as possible sources for microwaves. Following the stabilization time, there is almost complete reflection of the electron current. (no more than 1% propagates to the downstream end of the drift tube). The stabilization time of the potential corresponds roughly to one crossing time for the electron in the drift tube. Our results are in complete agreement with both theory and experiments [2] which have shown that when no ion source is present, the propagated current should be and in fact is always below the limiting value.

In a different run, with the same parameters, we provide an unlimited proton source at the injection boundary, having a mass ratio of $m_i/m_e = 25$. The emission is assumed to be space-charge limited. The total simulation time is 6 nsec, more than sufficient for the system to achieve a dynamic steady state. We have obtained both expected and unexpected results. In agreement with theory and experiments, most of the electron current ($\approx$80%) propagates to the downstream end of the tube (Fig. 5) and ions having energies several times the injected energy V_o, are observed (Fig. 6). Also, synchronous propagation of the electrons and the fast ions is evident, suggesting a strong electron-ion coupling.

Contrary to expectations, the virtual cathode does not display a clear motion downstream the drift tube. Rather, it has an irregular shape, changing continuously with time. Obviously, the most interesting results are those which have not been predicted by any existing analytical theory. First, the whole ion energy spectrum (the number of ions in different energy ranges), has been obtained, as a function of time (Fig. 6). Second, an unexpected feature, the formation of "virtual anodes" is observed, identified as short-lived regions of positive electrostatic potential (Fig. 7). They are due to the deceleration and bunching of ions in the region between the virtual cathode and the downstream end of the tube. A virtual anode is capable of further accelerating the ions towards the downstream end of the drift tube. It also accelerates the incoming electrons. This suggests the following mechanism for collective ion acceleration: first the incoming electrons are slowed down and transfer their energy to the initially slow ions, in the energy range $0\text{-}V_o$. Then, those ions form a "virtual anode", which accelerates the electrons. The virtual anode and the accelerated electrons further accelerate a smaller number of ions. This process can repeat itself, given a long enough e-beam pulse duration and a long enough drift tube. This picture is further strengthened by the ion energy spectra and their time derivatives (Figs. 6 and 8). First, one can see that the number of slow ions ($0\text{-}V_o$) is continuously increased by the incoming e-beam. Then the slower ions gradually transfer their energy to faster ions. More details can be found in Ref. 7. Obviously with these and other diagnostics, our particle simulation code is capable of following in detail the CIA mechanisms.

IV. CONCLUSIONS

Collective ion acceleration (CIA) is a complex phenomenon. We have built a computer simulation model including the dynamics of electrons and ions simultaneously which can be used to optimize the ion energy gain in present CIA experiments. A thorough parametric investigation of CIA is underway as a function of J_e^{inj}, V_o, d and other physical quantities. With our code, we have been able to identify an unexpected phenomena, the formation of short-lived "virtual anodes", capable of accelerating ions and electrons to high energies. Preliminary simulations show good qualitative agreement with experimental results.

In the absence of a self-consistent time-dependent analytical theory, it seems to us that the computer simulation model is an indispensable tool for the explanation and guidance of future CIA experiments. Our model can also be used to explain the fast ion energy spectrum observed in laser produced plasma experiments. The fast ions are a result of collective acceleration by the high energy electrons emerging from the laser absorption layer. The model can be used to relate the fast ion spectrum to the electron spectrum for diagnostic purposes.

ACKNOWLEDGMENTS

It is a pleasure to acknowledge the benefit of useful discussions with Dr. W. W. Destler.

Contract N00014-80C-0050

This research was supported by the Office of Naval Research under the auspices of the University of Maryland-Naval Research Laboratory Joint Program in Plasma Physics. The research by one of the authors (H.S.U) was supported by the Independent Research Fund at the Naval Surface Weapons Center.

REFERENCES

1. Proceedings of the Heavy Ion Fusion Workshop, Argonne National Laboratory, Argonne, Illinois, September 19-26, 1978.

2. W. W. Destler et al., J. Appl. Phys. 50, 3015 (1979).

3. R. Williams, Bull. Amer. Phys. Soc. 21, October 1976.

4. R. F. Hoeberling and D. N. Payton, J. Appl. Phys. 48, 2079 (1977).

5. J. S. Luce, Annals of N. Y. Acad. of Sci. 25, 2171 (1975).

6. H. S. Uhm and A. Sternlieb, submitted to J. Appl. Phys.

7. A Sternlieb and H. S. Uhm, "A Time-Dependent Study of Collective Ion Acceleration by Linear Electron Beams," University of Maryland Tech. Rep. #79-093, (1979).

8. A. Sternlieb et al., University of Maryland Tech. Rep. #79-060, (1979).

FIGURE CAPTIONS

Fig. 1: A schematic drawing of the simulated system; ϕ is the electrostatic potential, E_z is the electrostatic field, d is the length of the drift tube; the plasma source can be a proton rich thin foil or a puffed-in gas, ionized by the e-beam or by laser light.

Fig. 2: Flow chart of the computer code simulating the collective ion acceleration by linear electron beams. Space charge limited emission of ions is assumed.

Fig. 3: The configuration of the electrostatic potential well at several times, for the case with no ions present. Initially, there is a transient overshooting below V_o. Then, the depth of the potential well stabilizes and oscillates around the beam electron energy, V_o. J_e = 10 KA/cm^2, V_o = 1 MeV.

Fig. 4: The time variation of the virtual cathode amplitude ($|\phi^{min}(t)|$) for the case with no ions present. The potential stabilizes after approximately an electron crossing time along the drift tube.

Fig. 5: The time-dependent behavior of the various current components in the case with ions present. The notations are explained in the text. The injected e-beam current is 10 KA/cm^2.

Fig. 6: The time variation of the ion energy distribution function in four energy ranges: 0-1, 1-2, 2-3 and 3-4 MeV. The maximum energy observed is 4 MeV. The gradual transfer of energy from slower to faster ions is marked by sets of arrows. The units are logarithmic, arbitrary, but relatively correct.

Fig. 7: (a-e) The configuration of the electrostatic potential at intervals of 150 psec,

for the case with ions present. A conspicuous feature is the occasional appearance of short-lived regions of positive potential ("virtual anodes"), which are partially responsible for the ion acceleration.

Fig. 8: Time derivatives of the ion energy spectra in several energy ranges. The arrows show the gradual energy transfer from one range to the next.

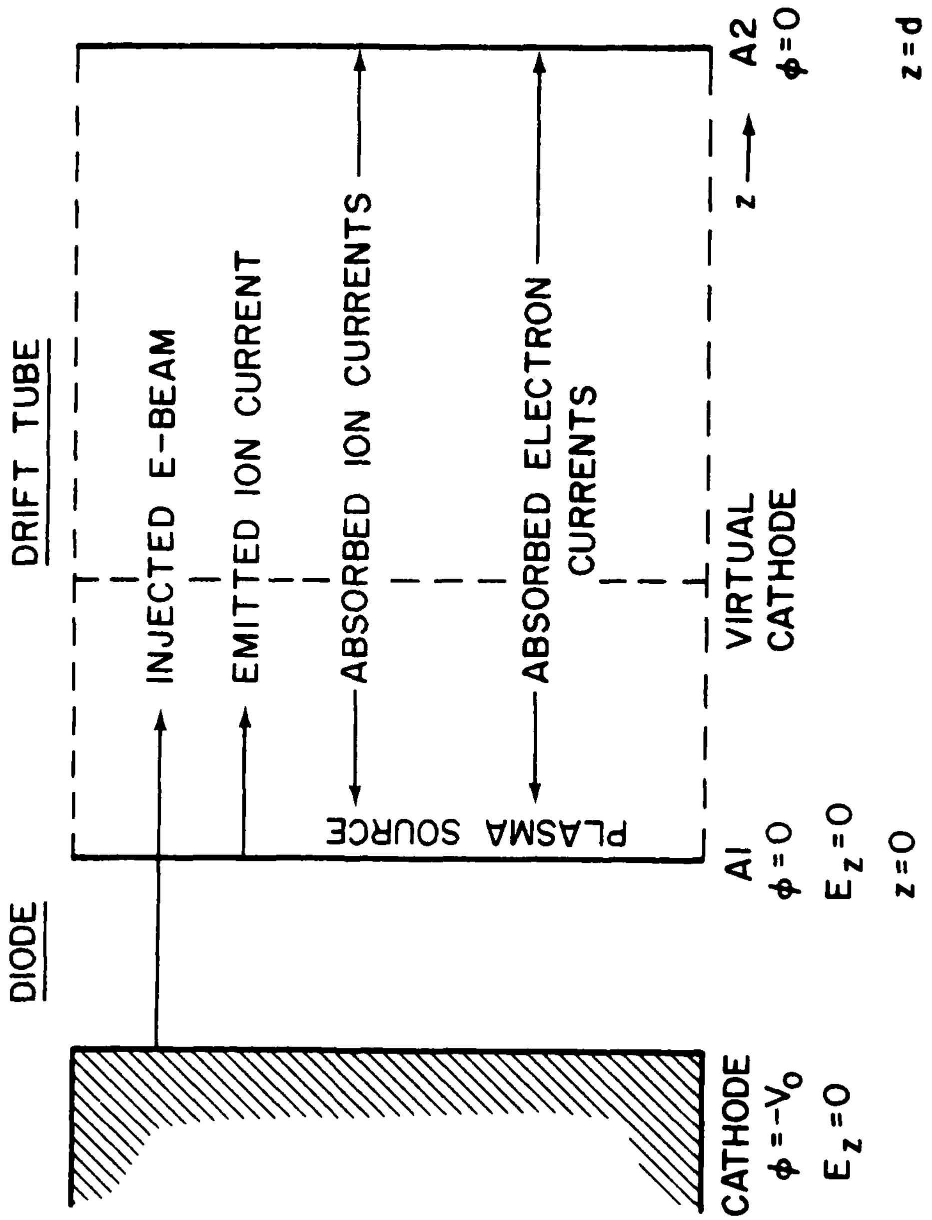

DIODE
DRIFT TUBE
INJECTED E-BEAM
EMITTED ION CURRENT
ABSORBED ION CURRENTS
ABSORBED ELECTRON CURRENTS
PLASMA SOURCE
VIRTUAL CATHODE
CATHODE
$\phi = -V_0$
$E_z = 0$
A1
$\phi = 0$
$E_z = 0$
$z = 0$
$z \longrightarrow$
A2
$\phi = 0$
$z = d$

Figure 1

FLOW CHART OF THE CODE (in C.G.S. Units)

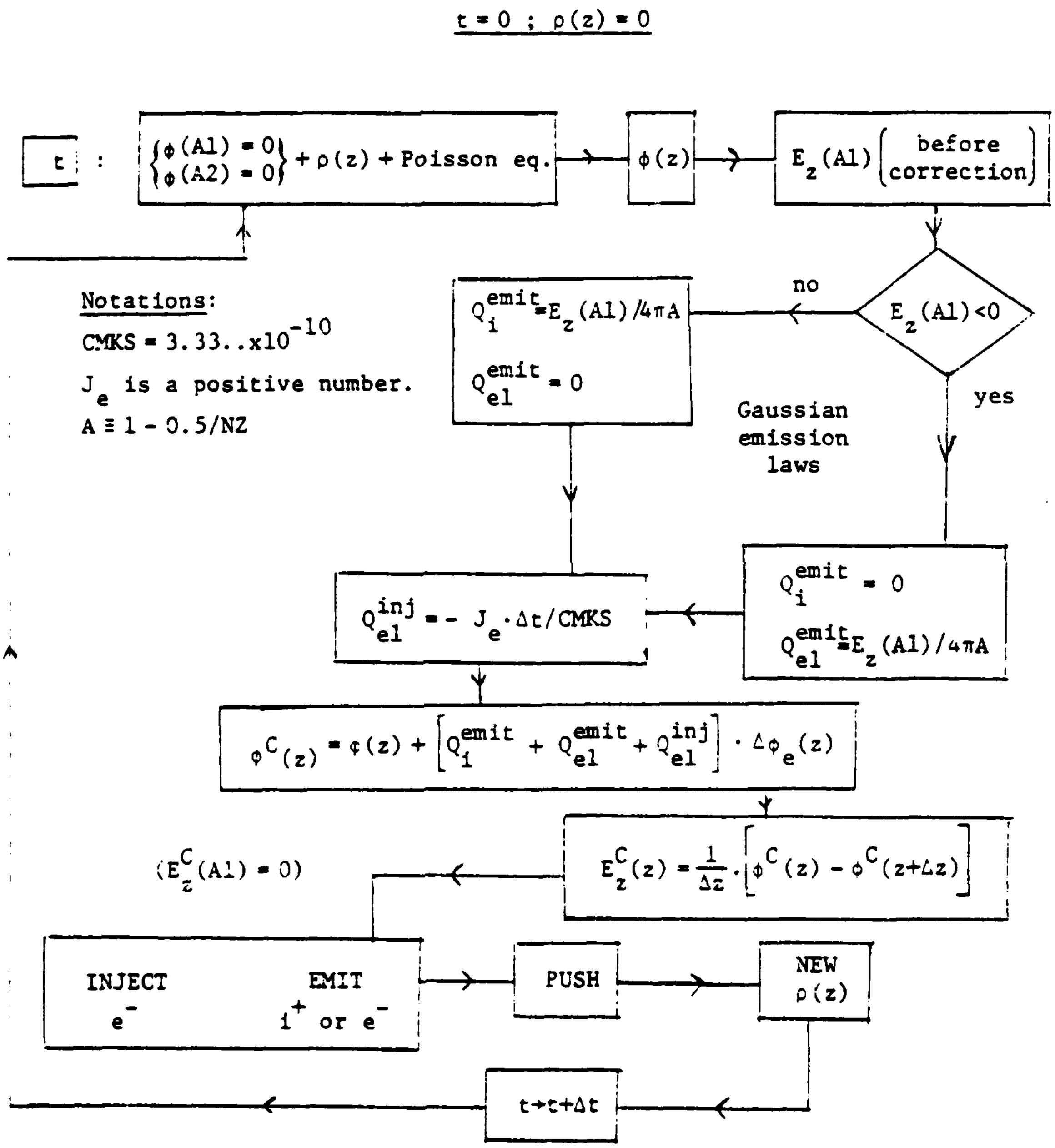

Figure 2

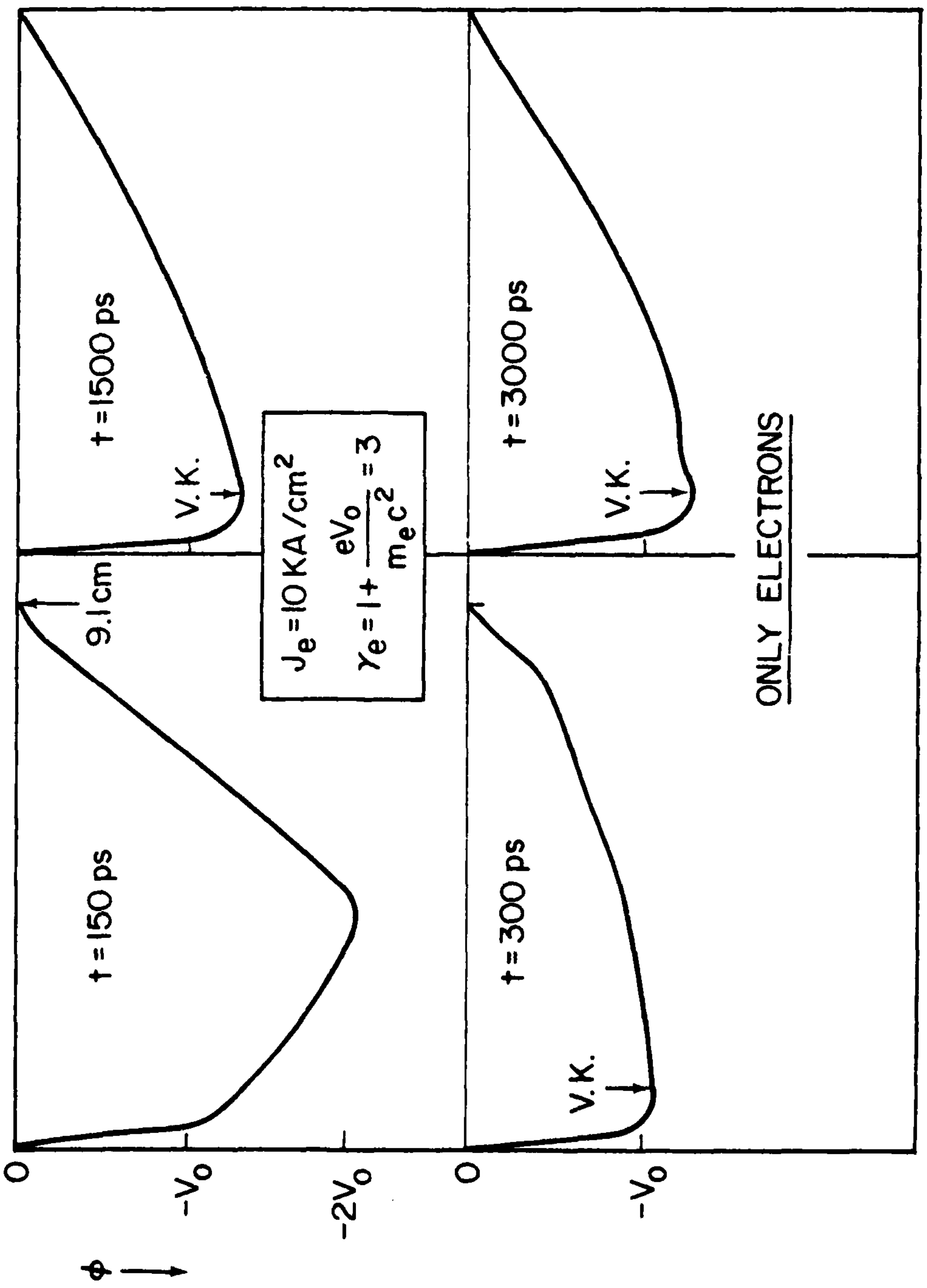

t = 150 ps
t = 1500 ps
t = 300 ps
t = 3000 ps
V.K.
V.K.
V.K.
9.1 cm
J_e = 10 KA/cm^2
γ_e = 1 + eV_o/(m_e c^2) = 3
ONLY ELECTRONS
0
-V_o
-2V_o
0
-V_o
φ

Figure 3

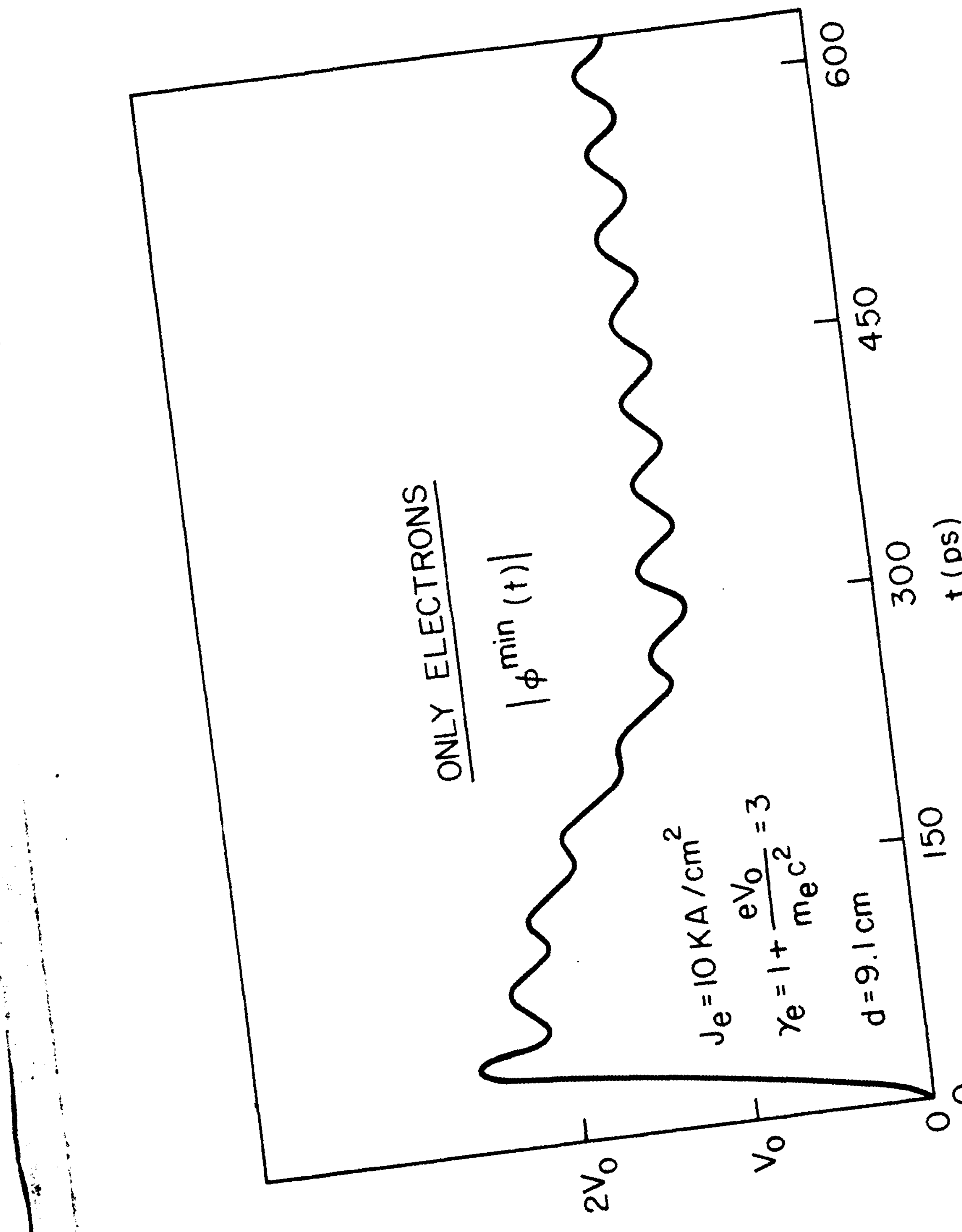
ONLY ELECTRONS
$|\phi^{min}(t)|$
$J_e = 10 KA/cm^2$
$\gamma_e = 1 + \frac{eV_0}{m_e c^2} = 3$
d=9.1 cm
$2V_0$
V_0
0
0
150
300
450
600
t (ps)

Figure 4

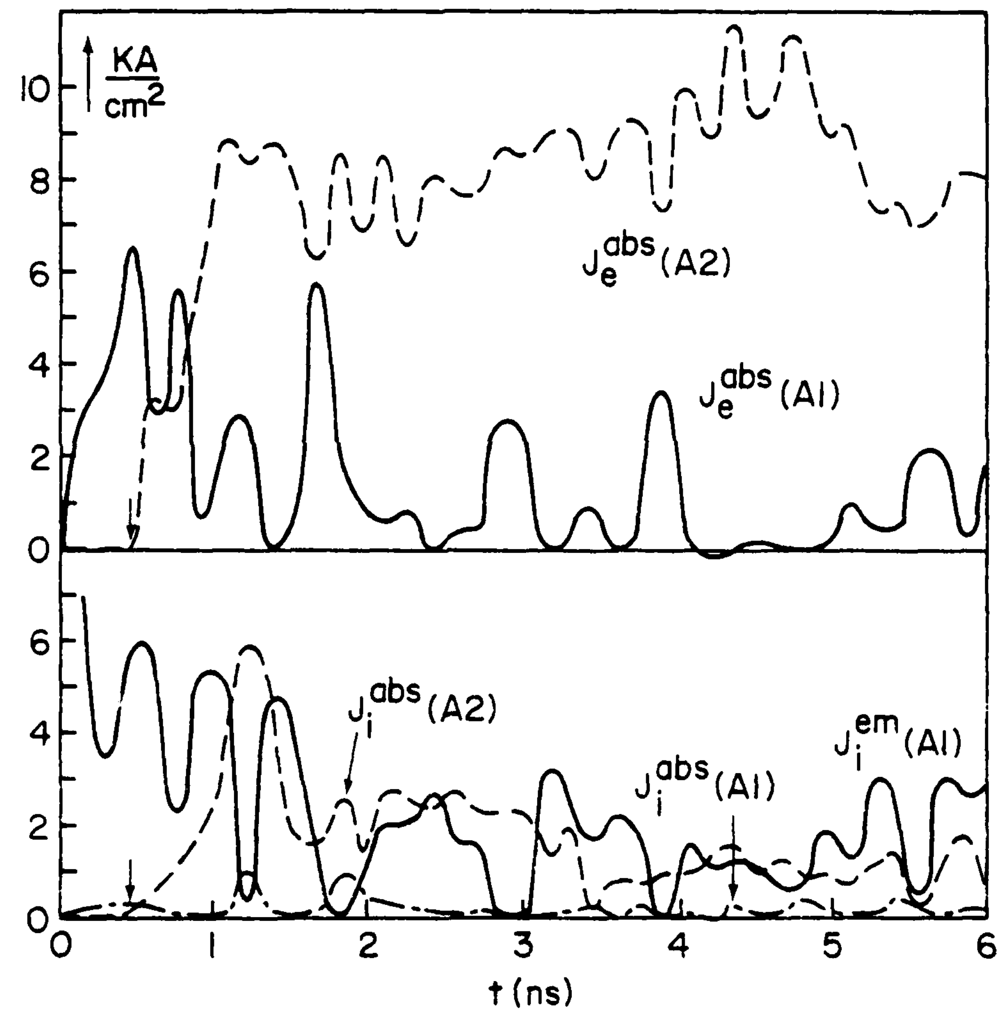
KA
cm2
10
8
6
4
2
0
6
4
2
0
0
1
2
3
4
5
6
t (ns)
J_e^abs (A2)
J_e^abs (A1)
J_i^abs (A2)
J_i^abs (A1)
J_i^em (A1)

Figure 5

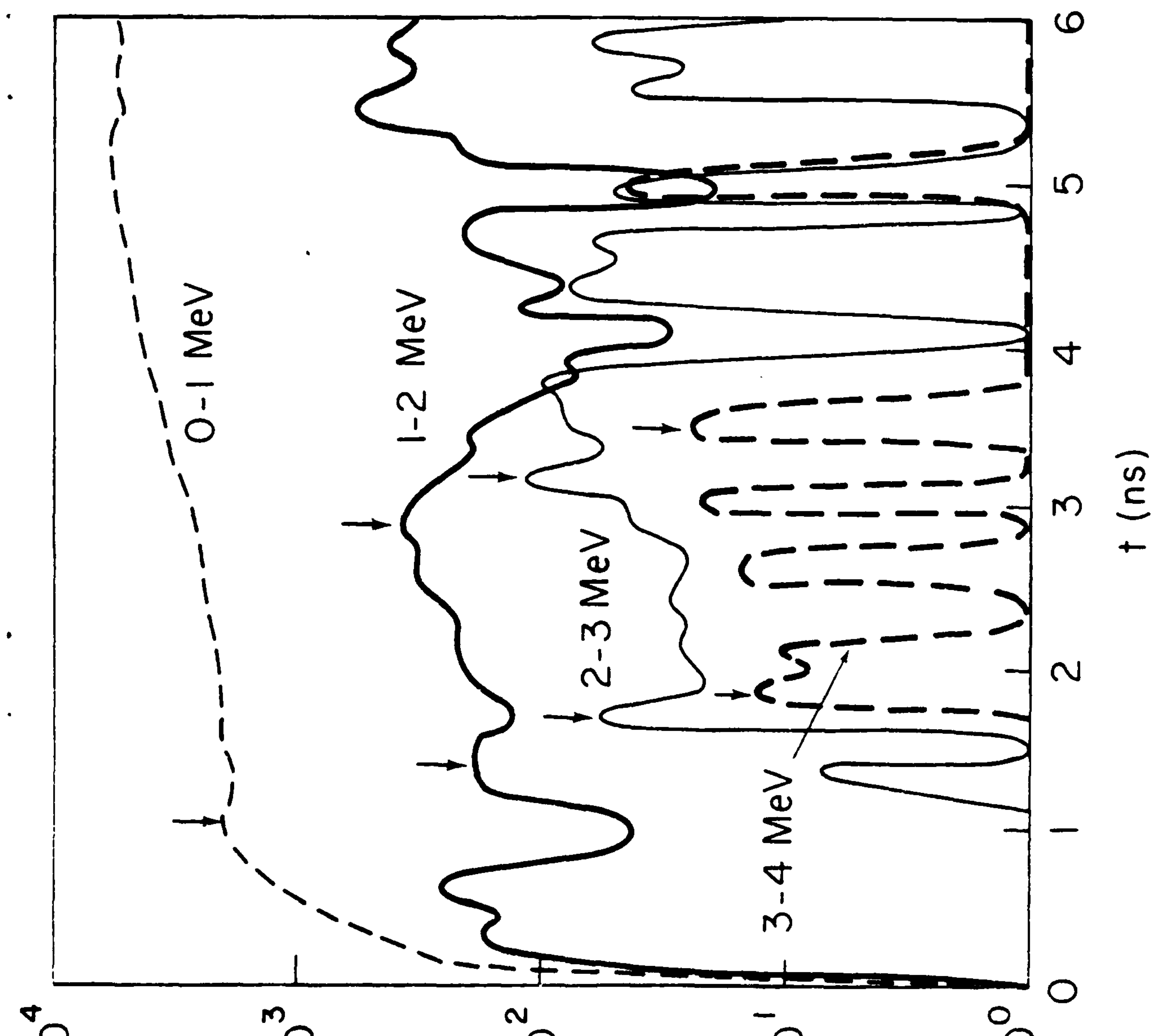

Figure 6

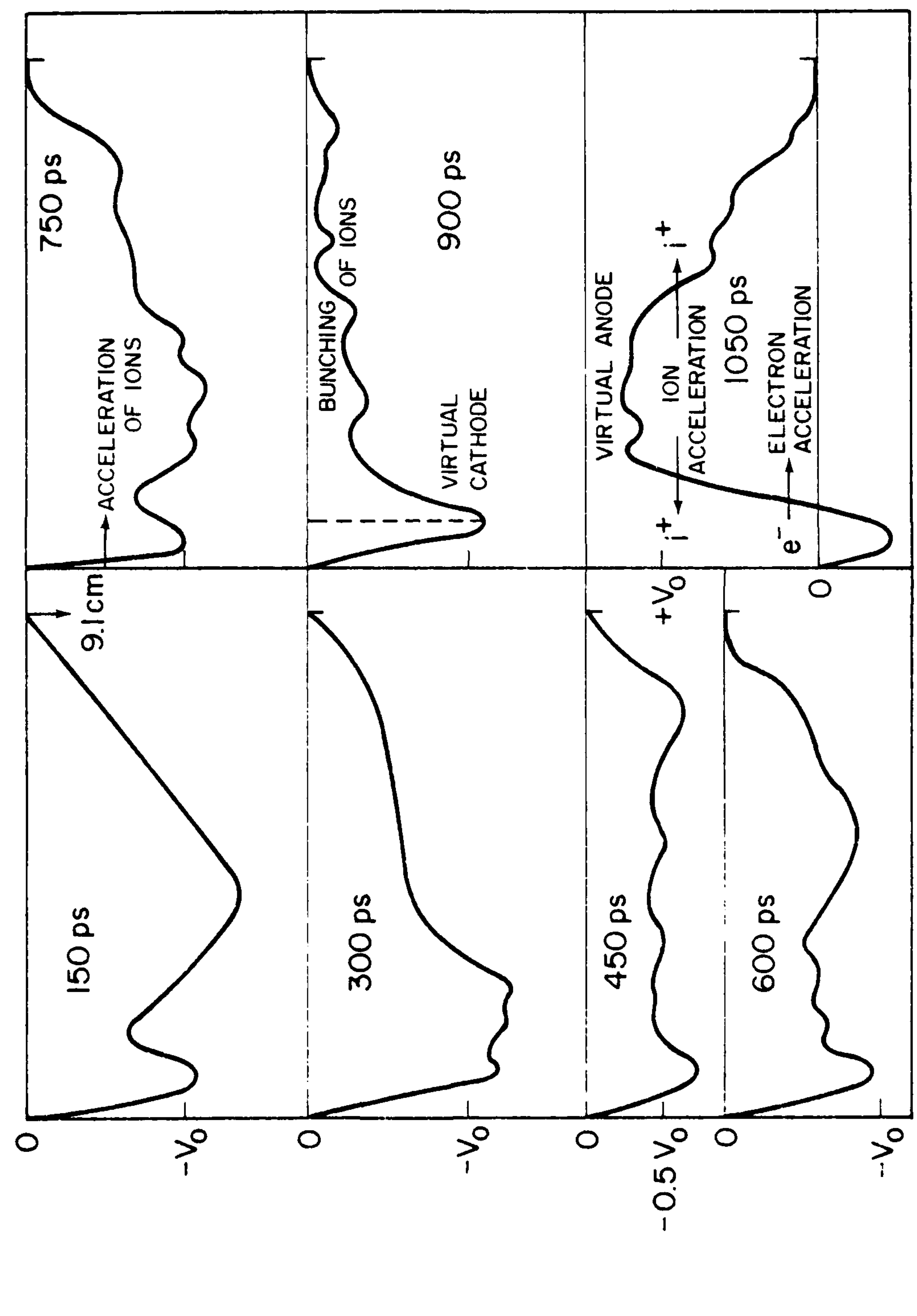

0
-V₀
0
-V₀
0
-0.5 V₀
0
-V₀
150 ps
300 ps
450 ps
600 ps
9.1 cm
+V₀
0
750 ps
ACCELERATION OF IONS
900 ps
BUNCHING OF IONS
VIRTUAL CATHODE
VIRTUAL ANODE
ION ACCELERATION
1050 ps
ELECTRON ACCELERATION
i+
i+
e-

Figure 7(a)

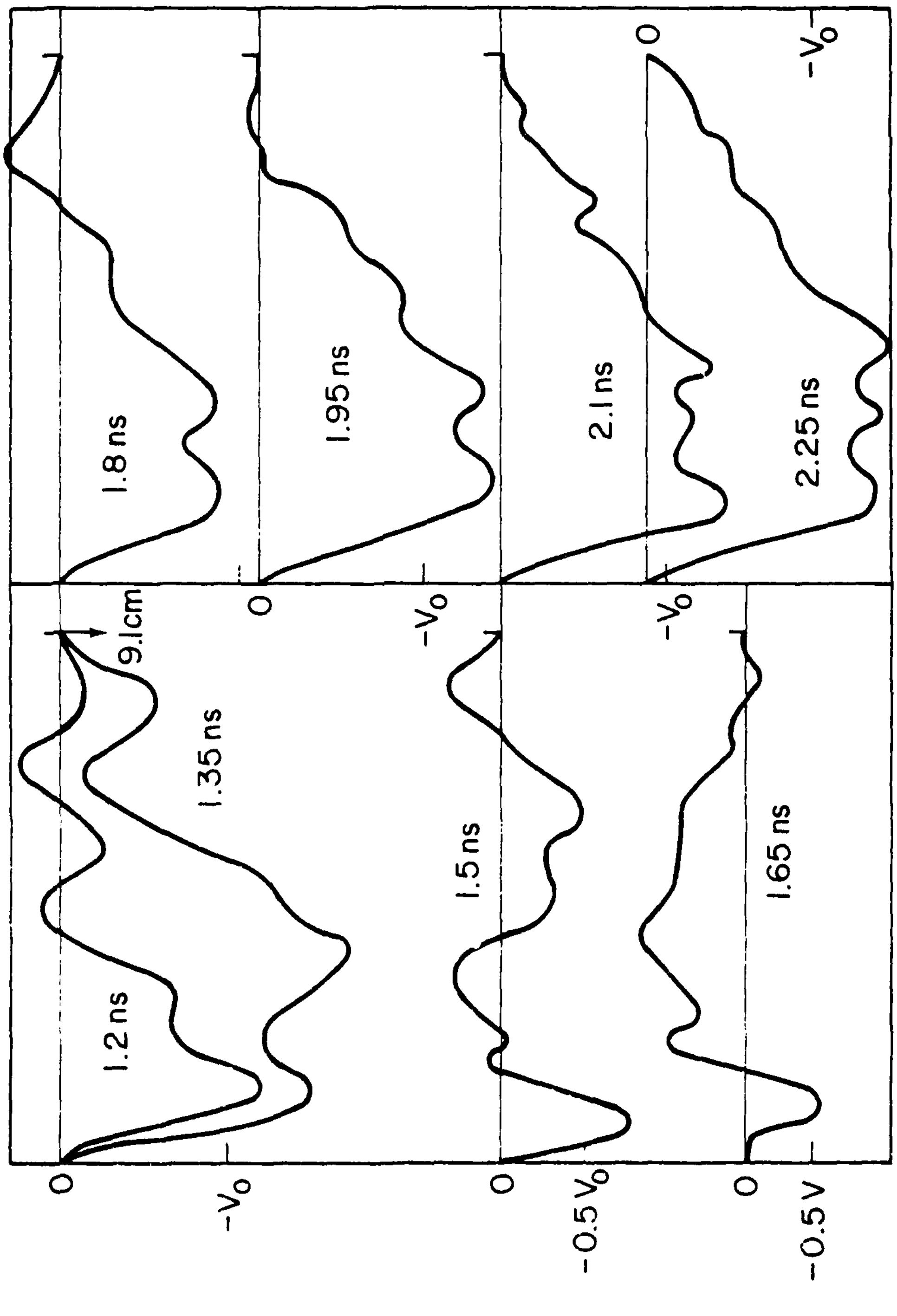
1.2 ns
1.35 ns
9.1cm
1.5 ns
1.65 ns
1.8 ns
1.95 ns
2.1 ns
2.25 ns
0
$-V_o$
$-0.5\,V_o$
$-0.5\,V$

Figure 7(b)

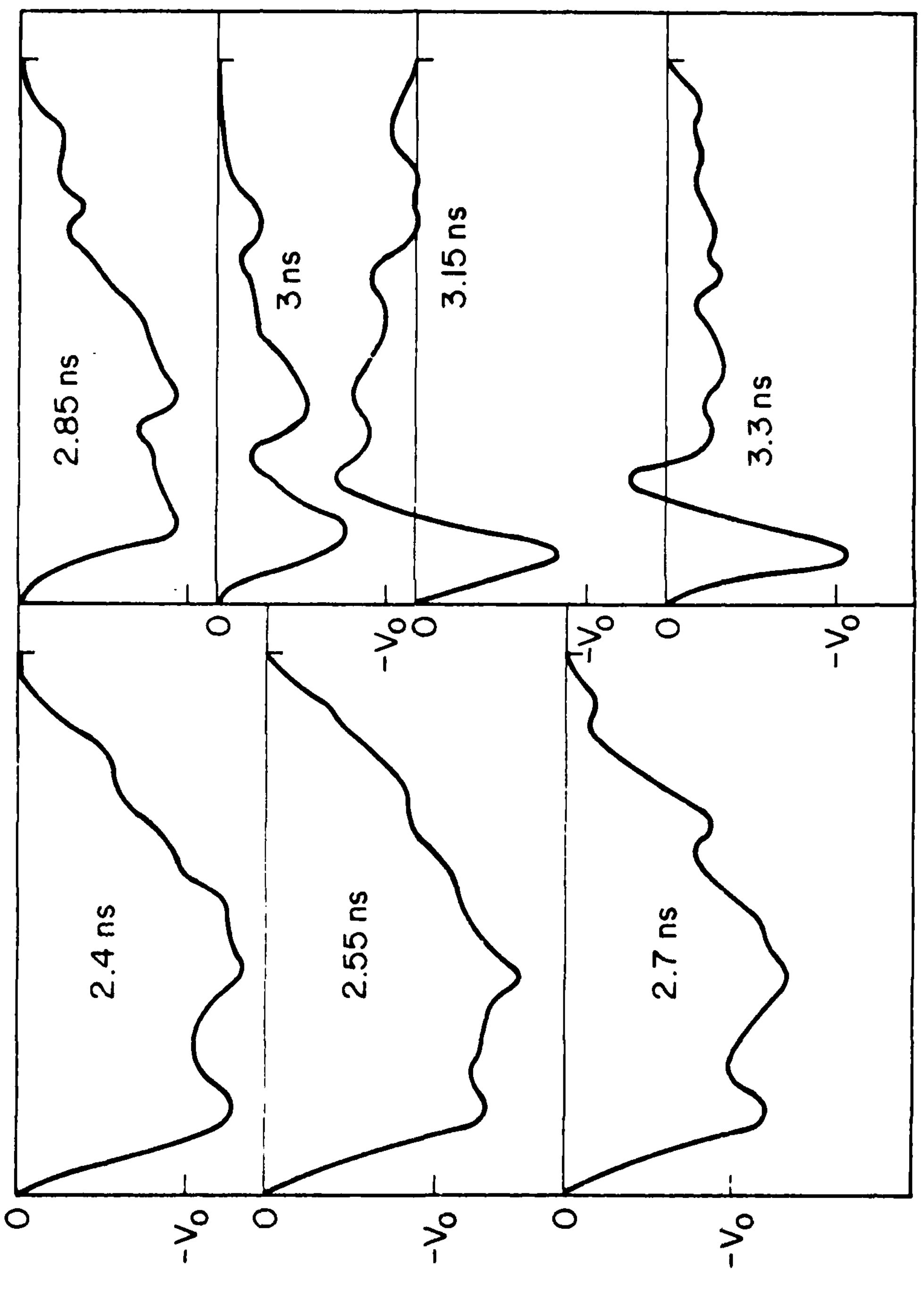

Figure 7(c)

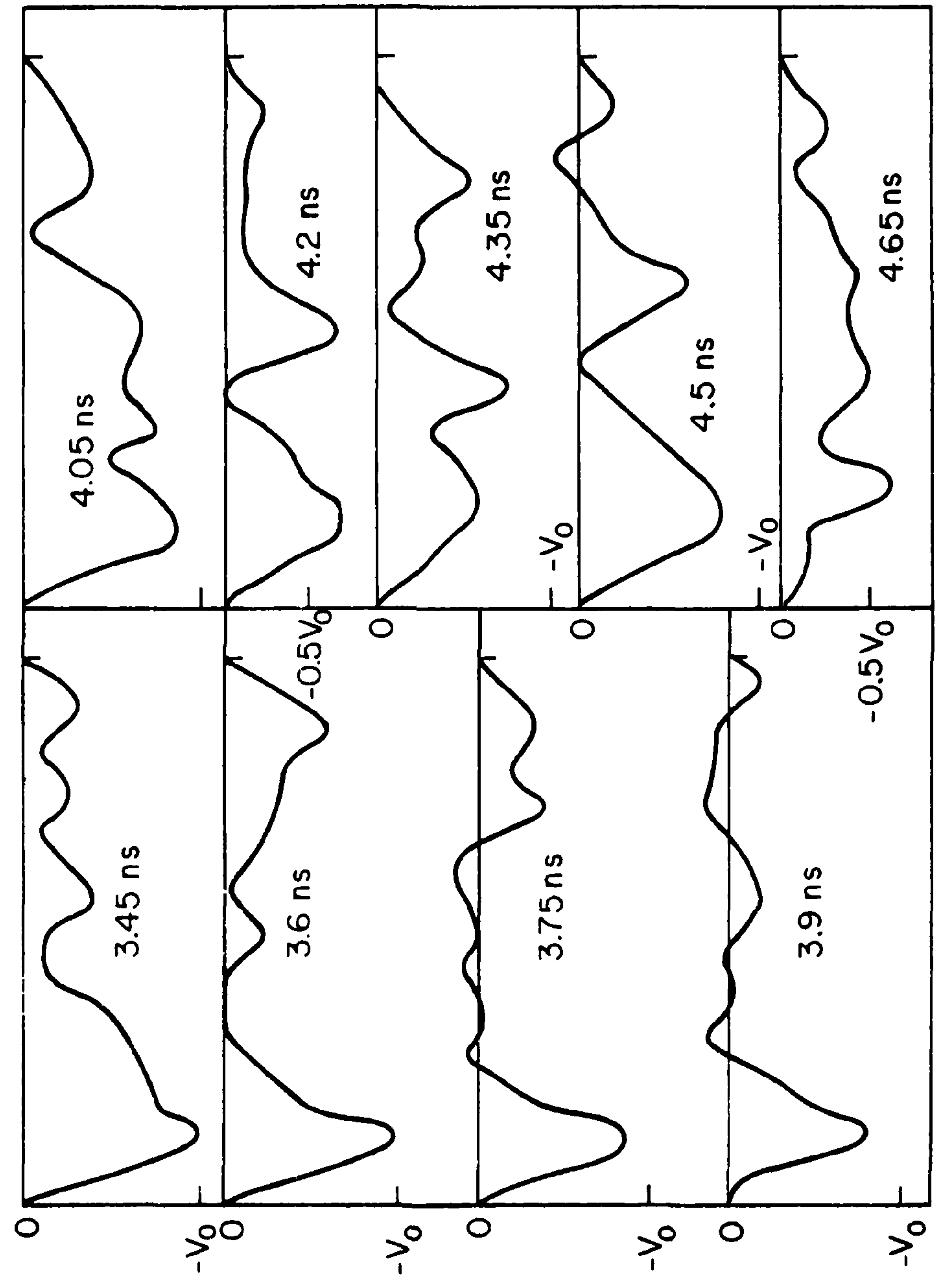

Figure 7(d)

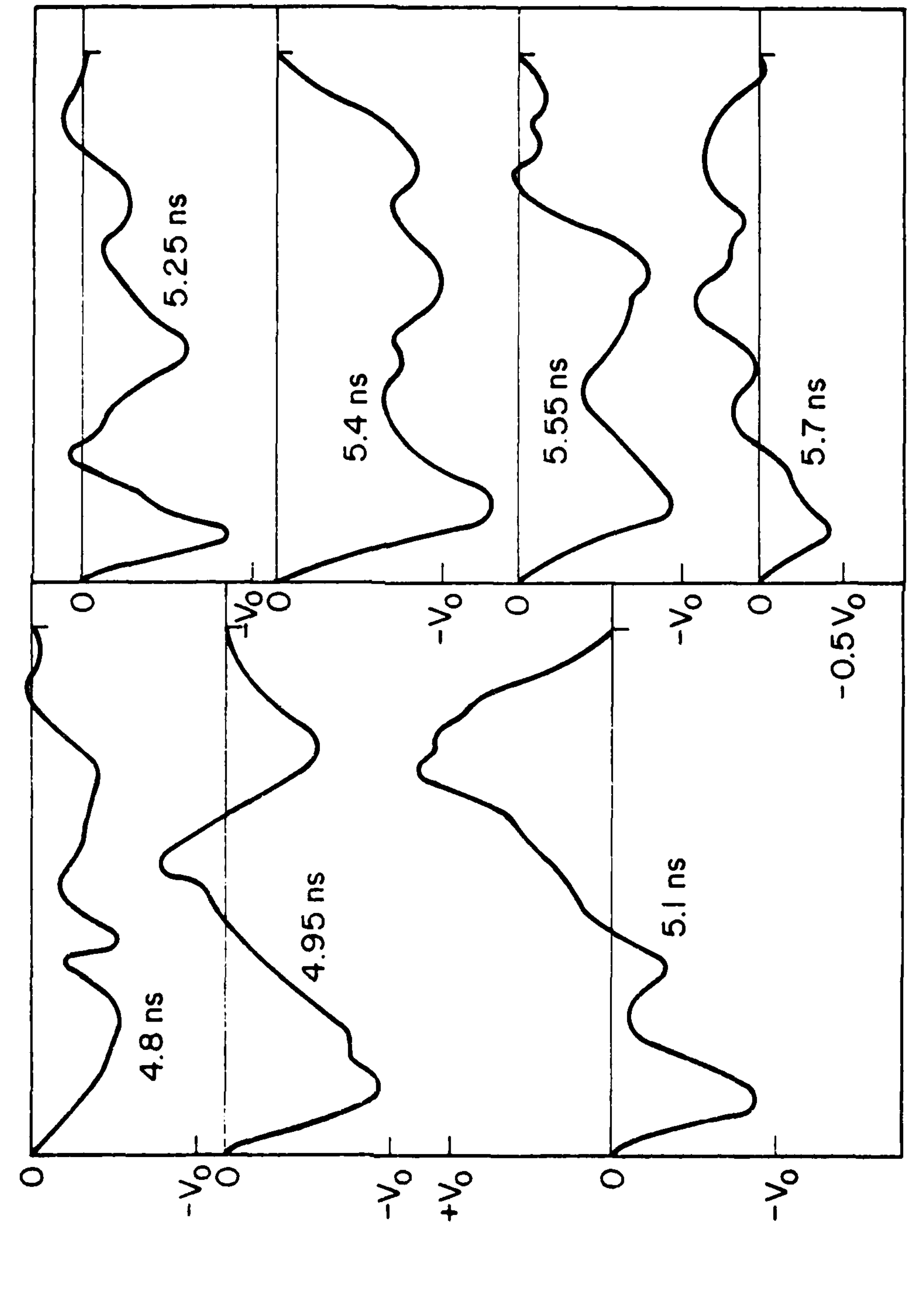

Figure 7(e)

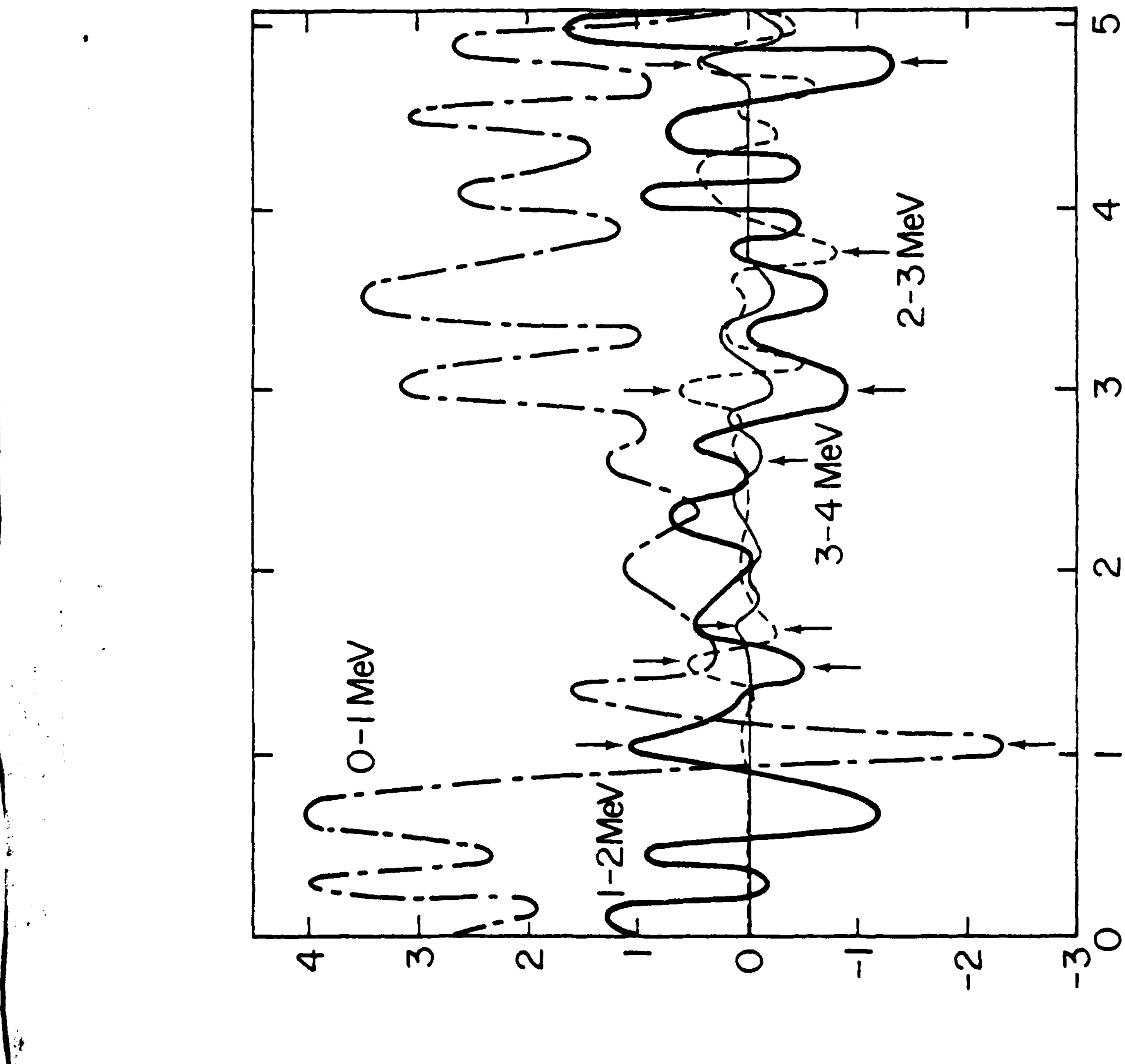

Figure 8